ACS central science

http://pubs.acs.org/journal/acscii

Research Article

Ordered Nanostructures in Thin Films of Precise Ion-Containing Multiblock Copolymers

Jinseok Park, Anne Staiger, Stefan Mecking, and Karen I. Winey*

Cite This: *ACS Cent. Sci.* 2022, 8, 388−393

Read Online

ACCESS | Metrics & More | Article Recommendations | Supporting Information

ABSTRACT: We demonstrate that ionic functionality in a multiblock architecture produces highly ordered and sub-3 nm nanostructures in thin films, including bicontinuous double gyroids. At 40 °C, precise ion-containing multiblock copolymers of poly(ethylene-*b*-lithium sulfosuccinate ester)$_n$ (PES*x*Li, x = 12 or 18) exhibit layered ionic assemblies parallel to the substrate. These ionic layers are separated by crystalline polyethylene blocks with the polymer backbones perpendicular to the substrate. Notably, above the melting temperature (T_m) of the polyethylene blocks, layered PES18Li thin films transform into a highly oriented double-gyroid morphology with the (211) plane (d_{211} = 2.5 nm) aligned parallel to the substrate. The cubic lattice parameter (a_{gyr}) of the double gyroid is 6.1 nm. Upon heating further above T_m, the double-gyroid morphology in PES18Li transitions into hexagonally packed cylinders with cylinders parallel to the substrate. These layered, double-gyroid, and cylinder nanostructures form epitaxially and spontaneously without secondary treatment, such as interfacial layers and solvent vapor annealing. When the film thickness is less than ~3a_{gyr}, double gyroids and cylinders coexist due to the increased confinement. For PES12Li above T_m, the layered ionic assemblies simply transform into disordered morphology. Given the chemical tunability of ion-functionalized multiblock copolymers, this study reveals a versatile pathway to fabricating ordered nanostructures in thin films.

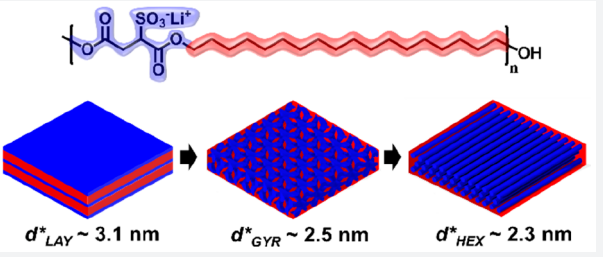

INTRODUCTION

Understanding the structural characteristics of polymer thin films is critical to numerous emerging technologies.[1,2] For example, self-assembly of block copolymer (*e.g.*, layer and cylinder) in thin films is essential to using these materials for nanolithography because the phase behavior can be significantly perturbed relative to the bulk behavior due to interfacial and confinement effects.[3−5] Also, conjugated polymers are widely studied in thin-film geometries because the alkyl chain crystallinity and $\pi-\pi$ stacked assemblies impact the electron transport properties,[6,7] which are valuable for transistors, light-emitting diodes, and photovoltaics.[8−11] Similarly, structure−property relationships of ion-containing polymer thin films have received significant interest for their ion transport abilities.[12−15] The perfluorinated sulfonic acid polymers (*e.g.*, Nafion) are among the most extensively studied ionomers for their applications in the catalyst layer of fuel cells and solar-fuel generators.[16,17] Specifically, the studies of Nafion have indicated that producing aligned morphologies of phase-separated sulfonic acid aggregates in a thin film can improve the proton transport properties or catalytic performance.[16,18−20]

Recent advances in polymer chemistry have enabled the precise segmentation of functional groups in polyethylene-based copolymers in contrast to the randomly distributed sulfonic acid groups of Nafion.[21−23] Notably, sulfonic acid groups placed at every 21st carbon of polyethylene blocks form well-defined ionic layers that achieve comparable proton conductivity to commercial Nafion.[24] In addition, strictly alternating multiblock copolymers composed of polyethylene and sulfosuccinate ester blocks with metal counterions (Li^+, Na^+, and Cs^+) have shown various ordered ionic aggregate morphologies, including layered, double-gyroid, and hexagonally packed cylinders.[25−28] Nanofabrication using the bicontinuous double-gyroid morphology is particularly important for applications in metamaterials and electrochemical devices.[29−33] While polyethylene-based multiblock copolymer ionomers are attractive platforms to explore as ion-conducting membranes and nanostructured templates, the ordered ionic assemblies and polyethylene backbones in these precise ionomers have not been studied in thin films. More broadly, relative to the diblock and triblock copolymer systems, thin-film studies are noticeably lacking for (AB)$_n$ alternating multiblock copolymers presumably due to the difficulties in achieving the strong segregation strength required for microphase separation.[34,35]

Received: December 28, 2021
Published: March 3, 2022

We now report precise ion-containing multiblock copolymers that produce desirable double gyroids and other ordered nanostructures in thin films with exceptional fidelity. The temperature-dependent thin-film morphologies are investigated by *in situ* grazing-incidence wide- and small-angle X-ray scattering (GIWAXS and GISAXS). Notably, within the ∼25−50 nm thick films, we observe highly oriented double-gyroid morphologies in a poly(ethylene-*b*-lithium sulfosuccinate ester)$_n$, where the cubic lattice parameter is only 6.1 nm. This gyroid morphology exhibits a thermotropic order-to-order transition into hexagonally packed cylinders with a lattice parameter of ∼2.7 nm. These ordered nanostructures with sub-3 nm domain spacings form spontaneously without any secondary treatment, such as neutral layers, top coats, and solvent vapor annealing.

RESULTS AND DISCUSSION

Precise ion-containing multiblock copolymers, poly(ethylene-*b*-lithium sulfosuccinate ester)$_n$ (PES*x*Li, x = 12 and 18), contain exactly x-methylene carbons strictly alternating with short polar blocks of lithium sulfosuccinate esters (Scheme 1).

Scheme 1. Chemical Structure of Precise Ion-Containing Multiblock Copolymers: (a) PES12Li (n = 55) and (b) PES18Li (n = 17)

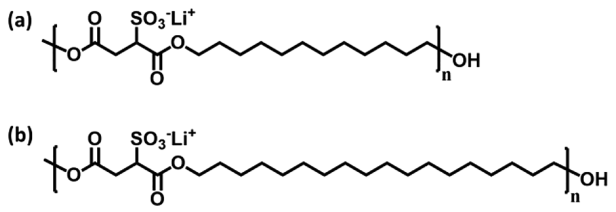

Note that these polymers are synthesized via step-growth polymerization of two monomers of fixed lengths, thereby achieving molecular weight monodispersity of the repeating blocks. The synthesis of materials, molecular weights, and bulk morphologies were previously reported.[28] End-group analysis using ^{1}H nuclear magnetic resonance spectroscopy determines that the molecular weights of PES12Li and PES18Li are 20 and 7.7 kg/mol, respectively.

In situ GIWAXS and GISAXS provide the structural characteristics of PES12Li in a 25 nm thin film. At 40 °C, in-plane scattering intensities at $q_y \approx 1.5$ Å^{-1} indicate that the polyethylene blocks crystallize into a hexagonal crystal with the chain axis perpendicular to the substrate (Figure 1a).[36,37] Above the melting point (T_m) at 140 °C, amorphous polyethylene blocks exhibit no preferential orientation as indicated by the broad and isotropic intensity ring at $q \approx 1.4$ Å^{-1} (Figure 1b). The melting transition of polyethylene coincides with changes in the small-angle scattering features originating from the polar blocks of lithium sulfosuccinate esters, namely, the ionic aggregates. *In situ* GISAXS experiments are performed to provide better resolution at $q < 0.6$ Å^{-1}. In Figure 1c, intensities along the q_z axis with a peak ratio (q/q^*) of 1:2 correspond to the ionic layers parallel to the substrate. The polar blocks of the PES12Li are expected to contact the −OH groups on the silicon substrate, while polyethylene blocks crystallize (see inset schematic in Figure 1a). In precisely functionalized polyethylenes synthesized by acyclic diene metathesis, chain folding accommodates both crystalline polyethylene and ionic layers.[37] Thus, the layer spacing of $2\pi/q^* = 2.5$ nm in PES12Li is the combined length of a polyethylene block (12 all-*trans* carbons, 1.4 nm) and two polar blocks. At 140 °C, GISAXS shows a disordered ionic aggregate morphology accompanying the amorphous polyethylene, as evidenced by the isotropic intensity ring ($q \approx 0.3$ Å^{-1}), Figure 1d. Thus, grazing-incidence X-ray scattering highlights the preferentially oriented ionic layers and polyethylene chain of PES12Li in thin films below T_m.

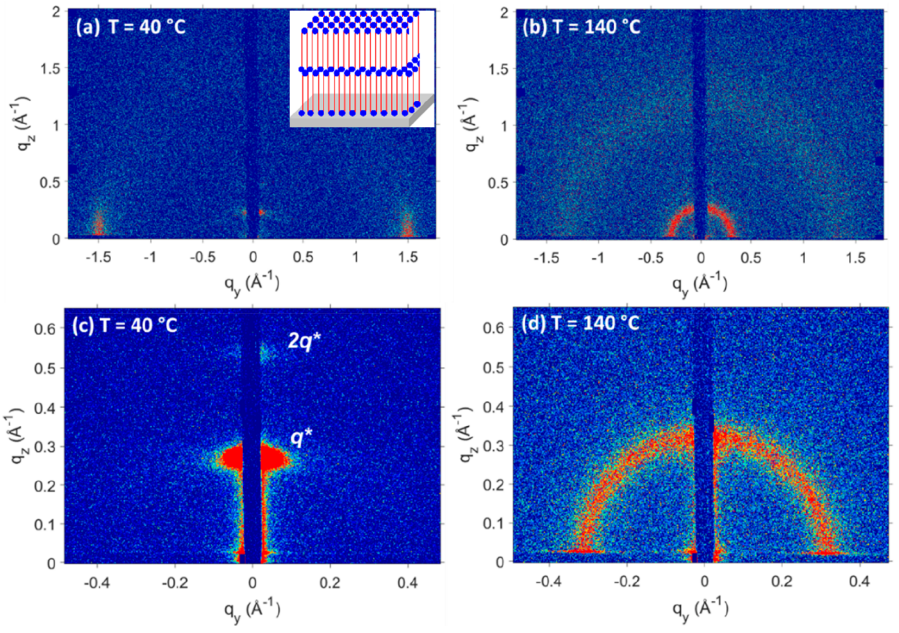

Figure 1. *In situ* 2D (a, b) GIWAXS and (c, d) GISAXS patterns of PES12Li thin films (∼25 nm thick) at 40 and 140 °C showing a transition from parallel layers to a disordered morphology. Exposure times are (a, b) 20 min, (c) 2 h, and (d) 1 h. Inset schematic in (a) represents the layered polar blocks (blue) separated by the crystalline polyethylene blocks (red).

https://doi.org/10.1021/acscentsci.1c01594
ACS Cent. Sci. 2022, 8, 388−393

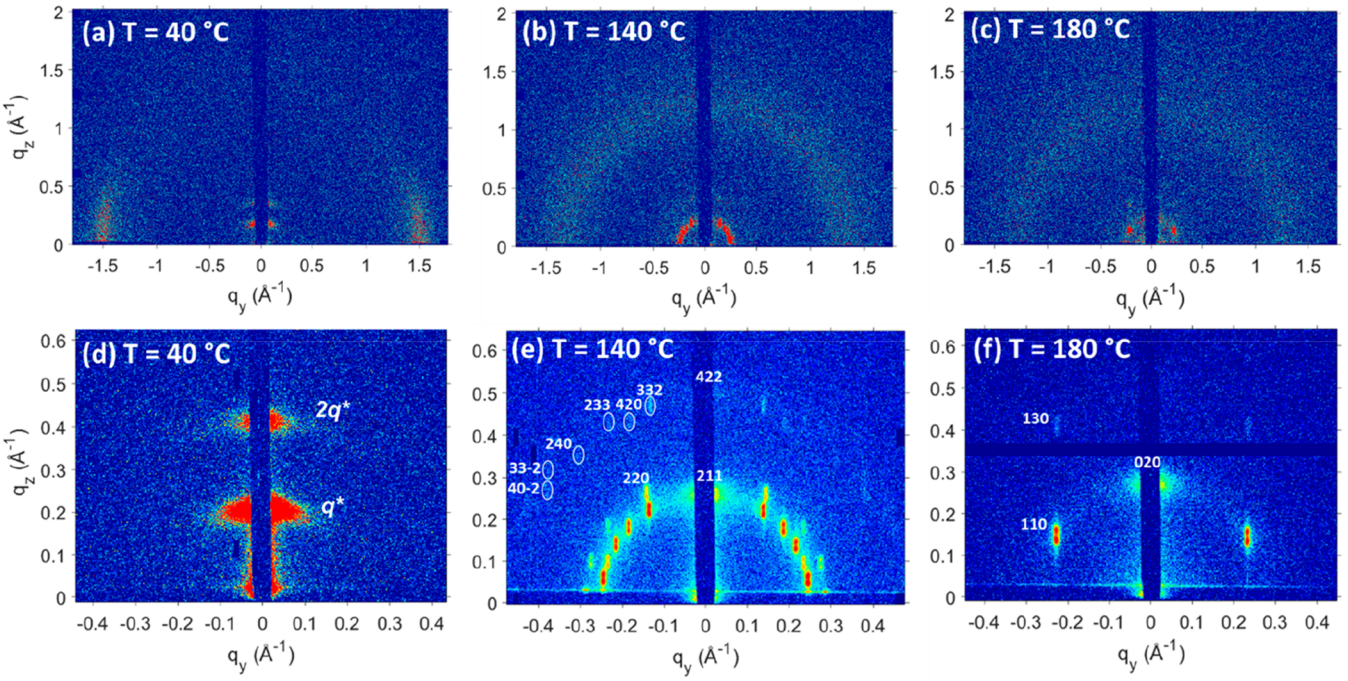

Figure 2. *In situ* 2D (a–c) GIWAXS and (d–f) GISAXS patterns of PES18Li thin films (~44 nm thick) at 40, 140, and 180 °C showing parallel layers, double gyroids, and hexagonal cylinders. Miller indexes in (e) and (f) are shown for the double gyroid and 2D orthorhombic lattice, respectively. Exposure times are (a–d) 20 min, (e) 3 h, and (f) 2 h.

While PES12Li and PES18Li are similar at 40 °C, PES18Li exhibits order to order transitions. The scattering intensities for PES18Li at $q_y \approx 1.5$ Å^{-1} arise from the vertically aligned polyethylene chains, and the out-of-plane scattering intensities with a peak ratio (q/q^*) of 1:2 and $q_z^* \approx 0.20$ Å^{-1} indicate parallel ionic layers with $d \approx 3.1$ nm (Figure 2a and 2d). This lattice parameter is 0.6 nm larger than that in PES12Li and consistent with the additional length of the alkyl block (18 all-trans carbons, 2.1 nm). The PES18Li thin film at 140 and 180 °C exhibits highly oriented double gyroids and hexagonally packed cylinders, respectively (Figure 2b and 2c). In Figure 2e, the GISAXS intensities are indexed for the cubic double-gyroid ($Ia\bar{3}d$) morphology where the (211) plane is preferentially oriented parallel to the substrate.[38,39] These peak assignments were made by calculating the scattered intensities for a double gyroid using GIXSGUI, see Figure S1.[40] The cubic lattice parameter of the double-gyroid morphology is a_{gyr} = 6.1 nm, corresponding to a film thickness of ~7a_{gyr} (~44 nm). At 180 °C, the gyroid morphology transitions into hexagonally packed cylinders oriented parallel to the substrate, as evidenced by the assigned peaks for the 2-dimensional orthorhombic lattice (Figure 2f). The calculated GISAXS profile, including both reflected and transmitted beams, is provided in Figure S2. The orthorhombic lattice parameters are a_{ortho} = 2.7 nm and b_{ortho} = 4.7 nm, and the film thickness (44 nm) is ~9b_{ortho}. The orthorhombic lattice is equivalent to a hexagonal lattice as shown in Figure S3.[41,42] Using the polar volume fraction (0.31) of PES18Li, we compute the cylinder diameter to be ~1.1 nm. Note that the transitions between the double-gyroid and hexagonally packed cylinder morphologies are reversible, and the double-gyroid morphology reforms upon cooling. This precise ion-containing multiblock copolymer exhibits an exceptional ability to produce highly oriented and sub-3 nm ordered nanostructures in thin films. Further, these ordered nanostructures are obtained spontaneously upon heating without any secondary treatment, such as interfacial layers and solvent vapor annealing.

We further investigate the stability of double gyroids in PES18Li thin films with increasing 2-dimensional confinement, *i.e.*, decreasing film thickness. Temperature-dependent ionic aggregate morphologies are determined from *in situ* GISAXS experiments for 17, 26, and 44 nm thick PES18Li films and summarized in Figure 3. The 2D scattering patterns collected in 10 °C increments are provided in Figures S4–S6. At all film thicknesses below 120 °C, ionic layers are aligned parallel to the substrate due to the crystalline polyethylene. For the 44 nm thick film, double gyroids exist at 130–160 °C and then

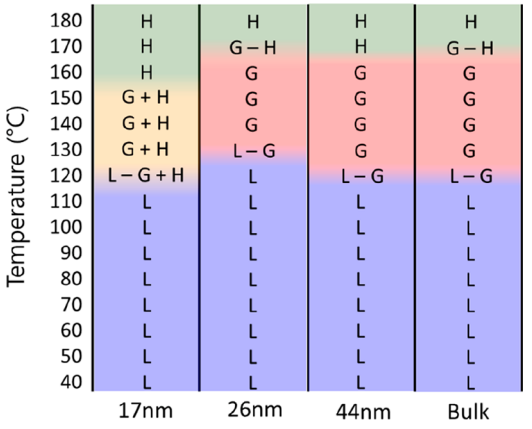

Figure 3. Temperature-dependent morphology diagram of PES18Li thin films with thicknesses of 17, 26, and 44 nm. Bulk morphologies are obtained from ref 28. Layered (L), double-gyroid (G), and hexagonally packed cylinders (H) morphologies of ionic assemblies are determined from the *in situ* GISAXS with temperature increments of 10 °C upon heating. See Figures S4–S6 for the corresponding 2D scattering patterns.

https://doi.org/10.1021/acscentsci.1c01594
ACS Cent. Sci. 2022, 8, 388–393

transition into cylinders upon heating, similar to the bulk behavior.[28] These order to order transitions are epitaxial with the differences of characteristics lengths < 0.2 nm at the transition temperatures (Figure S7). Highly oriented double gyroids are also identified within the 26 nm thick film, where the film thickness coincides with $\sim 4a_{gyr}$ or $\sim 10d_{211}$. In a further confined geometry (17 nm thick film), the double-gyroid and hexagonally packed cylinder morphologies coexist at 130−150 °C. The thin-film confinement significantly impacts the morphologies when the film thickness is on the order of a few lattice parameters, as widely observed in other block copolymer systems.[43,44] Here, we show that PES18Li spontaneously self-assembles into highly aligned double gyroids in thin films as thin as 26 nm, $\sim 4a_{gyr}$.

In previously studied diblock copolymers and giant surfactants, double gyroids exist in relatively thick films (>150 nm) to meet the commensurability of their large lattice parameters.[43,45] Alternatively, controlling interfacial layers with top coats and solvent vapor annealing can facilitate the formation of double gyroids in thinner films.[46−48] Recently, a disaccharide−atactic polypropylene conjugate showed double gyroids (a_{gyr} = 13.1 nm) in thin films (15−150 nm) on carbon-coated silicon substrates, suggesting hydrogen-bonding interaction of saccharides is a crucial factor in determining the morphology.[49] Here, we demonstrate that a precise ion-containing multiblock copolymer self-assembles into highly oriented double gyroids with a smaller lattice parameter of 6.1 nm in thin films (≥26 nm). We attribute these double-gyroid morphologies in thin films to (1) the precisely alternating $(AB)_n$ multiblock architecture with perfectly monodisperse block length and (2) the large interaction parameter between the blocks that drive microphase separation via ionic functionalities.

CONCLUSIONS

We investigated the structural characteristics of two precise ion-containing multiblock copolymers, poly(ethylene-*b*-lithium sulfosuccinate ester)$_n$. As-prepared thin films form layered ionic assemblies separated by the crystalline polyethylene blocks. The ionic layers are aligned parallel to the substrate, and the domain spacings are 2.5 and 3.1 nm for PES12Li and PES18Li, respectively. Importantly, PES18Li produces highly oriented double gyroids with a cubic lattice parameter (a_{gyr}) of just 6.1 nm in confined thin-film geometries with thicknesses of $\sim 4a_{gyr}$ and $7a_{gyr}$. A thinner film ($<3a_{gyr}$) resulted in a mixed morphology of double gyroids and hexagonally packed cylinders. In these polymer thin films under confinement, the formation of double gyroids is attributed to the strictly alternating lithium sulfosuccinate ester blocks that strongly interact to produce the double gyroids with the (211) plane (d_{211} = 2.5 nm) parallel to the substrate. In addition, we reveal that the multiblock copolymers with monodisperse block lengths can self-assemble into ordered nanostructures in thin films, which will expand their utility. Future studies may explore double gyroids in thin films by modulating the polymer chemistries, as well as develop the potential applications of these ion-containing multiblock copolymer thin films into ion transport membranes and nanopatterning templates.

EXPERIMENTAL SECTION

No unexpected and significant hazards or risks were encountered during the experimental procedures.

Preparation of Polymer Thin Films. Details of materials synthesis, ^{1}H NMR characterization, and gel-permeation chromatography have been reported previously.[28] Thin films were prepared by spin coating PES12Li (0.5 wt %) and PES18Li (0.3, 0.5, and 1.0 wt %) polymer solutions in methanol on a bare silicon wafer for 1 min at 6000 rpm under ambient conditions. Silicon wafers were UV−ozone cleaned and directly used without any post-treatment. The film thicknesses were measured using a F3−UV reflectometer equipped with a LS-DT2 light source and SS-5 stage (Filmetrics). All samples were dried at 50 °C for 24 h under vacuum prior to X-ray scattering experiments. The melting temperatures of bulk PES12Li and PES18Li are 73 and 117 °C, respectively, according to differential scanning calorimetry.

Grazing-Incidence X-ray Scattering. Grazing-incidence X-ray scattering experiments were performed using the Dual-source and Environmental X-ray Scattering (DEXS) facility at the University of Pennsylvania. The DEXS facility is equipped with a GeniX3D beam source (8.05 keV, Cu Kα, λ = 1.54 Å) and a PILATUS 1 M detector. The 190 and 375 mm sample-to-detector distances were used for the *in situ* grazing-incidence wide-angle (GIWAXS) and small-angle (GISAXS) experiments. The sample to detector distances were calibrated using AgBeh. The incident beam angle was 0.20° for all measurements.

For PES12Li (25 nm thick) and PES18Li (44 nm thick) samples, *in situ* GIWAXS and GISAXS experiments were performed at specific temperatures of 40, 140, and 180 °C with a heating rate of 10 °C/min and an equilibration time of 10 min. Exposure times are specified in the figure captions.

For PES18Li (17, 26, and 44 nm) samples, *in situ* GISAXS experiments were performed at 40−180 °C with a temperature interval of 10 °C upon heating. The heating rate was 10 °C/min with an equilibration time of 5 min at each temperature, and exposure times were 20 min for all measurements. The assignments of the Miller indexes for 2D scattering patterns were made using GIXSGUI.[40]

ASSOCIATED CONTENT

Supporting Information

The Supporting Information is available free of charge at https://pubs.acs.org/doi/10.1021/acscentsci.1c01594.

GISAXS 2D scattering patterns of PES18Li for double gyroids and hexagonally packed cylinders; schematics for hexagonally packed cylinders and corresponding Miller indexes in hexagonal lattice vectors; full *in situ* GISAXS 2D scattering patterns of 17, 26, and 44 nm thick PES18Li thin films (PDF)

AUTHOR INFORMATION

Corresponding Author

Karen I. Winey − *Department of Materials Science and Engineering and Department of Chemical and Biomolecular Engineering, University of Pennsylvania, Philadelphia, Pennsylvania 19104, United States;* orcid.org/0000-0001-5856-3410; Email: winey@seas.upenn.edu

Authors

Jinseok Park − *Department of Materials Science and Engineering, University of Pennsylvania, Philadelphia, Pennsylvania 19104, United States;* orcid.org/0000-0002-0389-9707

https://doi.org/10.1021/acscentsci.1c01594
ACS Cent. Sci. 2022, 8, 388−393

Anne Staiger − *Department of Chemistry, University of Konstanz, 78457 Konstanz, Germany;* orcid.org/0000-0002-6103-4402

Stefan Mecking − *Department of Chemistry, University of Konstanz, 78457 Konstanz, Germany;* orcid.org/0000-0002-6618-6659

Complete contact information is available at: https://pubs.acs.org/10.1021/acscentsci.1c01594

Notes

The authors declare no competing financial interest.

■ ACKNOWLEDGMENTS

J.P. and K.I.W. acknowledge funding by the NSF DMR (1904767). J.P. and K.I.W. also acknowledge NSF MRSEC (17-20530), NSF MRI (17-25969), and ARO DURIP grants (W911NF-17-1-0282) for the Dual Source and Environmental X-ray Scattering facility at the University of Pennsylvania. Funding by the Baden-Württemberg Foundation (project "PRICON") is gratefully acknowledged. We also acknowledge access to the National Synchrotron Light Source II (beamline 11-BM, Brookhaven National Laboratory) and note that those results were consistent with our more extensive in-house X-ray scattering experiments.

■ REFERENCES

(1) Frank, C. W.; Rao, V.; Despotopoulou, M. M.; Pease, R. F. W.; Hinsberg, W. D.; Miller, R. D.; Rabolt, J. F. Structure in Thin and Ultrathin Spin-Cast Polymer Films. *Science* **1996**, *273*, 912−915.

(2) Russell, T. P.; Chai, Y. 50th Anniversary Perspective: Putting the Squeeze on Polymers: A Perspective on Polymer Thin Films and Interfaces. *Macromolecules* **2017**, *50*, 4597−4609.

(3) Huang, E.; Rockford, L.; Russell, T. P.; Hawker, C. J. Nanodomain Control in Copolymer Thin Films. *Nature* **1998**, *395*, 757−758.

(4) Fasolka, M. J.; Mayes, A. M. Block Copolymer Thin Films:Physics and Applications. *Annu. Rev. Mater. Res.* **2001**, *31*, 323−355.

(5) Hamley, I. W. Ordering in Thin Films of Block Copolymers: Fundamentals to Potential Applications. *Prog. Polym. Sci.* **2009**, *34*, 1161−1210.

(6) Huang, Y.; Kramer, E. J.; Heeger, A. J.; Bazan, G. C. Bulk Heterojunction Solar Cells: Morphology and Performance Relationships. *Chem. Rev.* **2014**, *114*, 7006−7043.

(7) Lu, L.; Zheng, T.; Wu, Q.; Schneider, A. M.; Zhao, D.; Yu, L. Recent Advances in Bulk Heterojunction Polymer Solar Cells. *Chem. Rev.* **2015**, *115*, 12666−12731.

(8) Di, C.; Liu, Y.; Yu, G.; Zhu, D. Interface Engineering: An Effective Approach toward High-Performance Organic Field-Effect Transistors. *Acc. Chem. Res.* **2009**, *42*, 1573−1583.

(9) Fang, J.; Wallikewitz, B. H.; Gao, F.; Tu, G.; Müller, C.; Pace, G.; Friend, R. H.; Huck, W. T. S. Conjugated Zwitterionic Polyelectrolyte as the Charge Injection Layer for High-Performance Polymer Light-Emitting Diodes. *J. Am. Chem. Soc.* **2011**, *133*, 683−685.

(10) Zhao, X.; Zhan, X. Electron Transporting Semiconducting Polymers in Organic Electronics. *Chem. Soc. Rev.* **2011**, *40*, 3728−3743.

(11) Yip, H. L.; Jen, A. K. Y. Recent Advances in Solution-Processed Interfacial Materials for Efficient and Stable Polymer Solar Cells. *Energy Environ. Sci.* **2012**, *5*, 5994−6011.

(12) Sharon, D.; Bennington, P.; Dolejsi, M.; Webb, M. A.; Dong, B. X.; De Pablo, J. J.; Nealey, P. F.; Patel, S. N. Intrinsic Ion Transport Properties of Block Copolymer Electrolytes. *ACS Nano* **2020**, *14*, 8902−8914.

(13) Lettow, J. H.; Kaplan, R. Y.; Nealey, P. F.; Rowan, S. J. Enhanced Ion Conductivity through Hydrated, Polyelectrolyte-Grafted Cellulose Nanocrystal Films. *Macromolecules* **2021**, *54*, 6925−6936.

(14) Sharon, D.; Bennington, P.; Webb, M. A.; Deng, C.; De Pablo, J. J.; Patel, S. N.; Nealey, P. F. Molecular Level Differences in Ionic Solvation and Transport Behavior in Ethylene Oxide-Based Homopolymer and Block Copolymer Electrolytes. *J. Am. Chem. Soc.* **2021**, *143*, 3180−3190.

(15) Zhao, Q.; Bennington, P.; Nealey, P. F.; Patel, S. N.; Evans, C. M. Ion Specific, Thin Film Confinement Effects on Conductivity in Polymerized Ionic Liquids. *Macromolecules* **2021**, *54*, 10520.

(16) Kusoglu, A.; Weber, A. Z. New Insights into Perfluorinated Sulfonic-Acid Ionomers. *Chem. Rev.* **2017**, *117*, 987−1104.

(17) Dudenas, P. J.; Kusoglu, A. Evolution of Ionomer Morphology from Dispersion to Film: An In Situ X-Ray Study. *Macromolecules* **2019**, *52*, 7779−7785.

(18) Hickner, M. A.; Pivovar, B. S. The Chemical and Structural Nature of Proton Exchange Membrane Fuel Cell Properties. *Fuel Cells* **2005**, *5*, 213−229.

(19) Modestino, M. A.; Kusoglu, A.; Hexemer, A.; Weber, A. Z.; Segalman, R. A. Controlling Nafion Structure and Properties via Wetting Interactions. *Macromolecules* **2012**, *45*, 4681−4688.

(20) Kusoglu, A.; Kushner, D.; Paul, D. K.; Karan, K.; Hickner, M. A.; Weber, A. Z. Impact of Substrate and Processing on Confinement of Nafion Thin Films. *Adv. Funct. Mater.* **2014**, *24*, 4763−4774.

(21) Buitrago, C. F.; Jenkins, J. E.; Opper, K. L.; Aitken, B. S.; Wagener, K. B.; Alam, T. M.; Winey, K. I. Room Temperature Morphologies of Precise Acid-and Ion-Containing Polyethylenes. *Macromolecules* **2013**, *46*, 9003−9012.

(22) Trigg, E. B.; Tiegs, B. J.; Coates, G. W.; Winey, K. I. High Morphological Order in a Nearly Precise Acid-Containing Polymer and Ionomer. *ACS Macro Lett.* **2017**, *6*, 947−951.

(23) Paren, B. A.; Thurston, B. A.; Kanthawar, A.; Neary, W. J.; Kendrick, A.; Maréchal, M.; Kennemur, J. G.; Stevens, M. J.; Frischknecht, A. L.; Winey, K. I. Fluorine-Free Precise Polymer Electrolyte for Efficient Proton Transport: Experiments and Simulations. *Chem. Mater.* **2021**, *33*, 6041−6051.

(24) Trigg, E. B.; Gaines, T. W.; Maréchal, M.; Moed, D. E.; Rannou, P.; Wagener, K. B.; Stevens, M. J.; Winey, K. I. Self-Assembled Highly Ordered Acid Layers in Precisely Sulfonated Polyethylene Produce Efficient Proton Transport. *Nat. Mater.* **2018**, *17*, 725−731.

(25) Yan, L.; Häußler, M.; Bauer, J.; Mecking, S.; Winey, K. I. Monodisperse and Telechelic Polyethylenes Form Extended Chain Crystals with Ionic Layers. *Macromolecules* **2019**, *52*, 4949−4956.

(26) Yan, L.; Rank, C.; Mecking, S.; Winey, K. I. Gyroid and Other Ordered Morphologies in Single-Ion Conducting Polymers and Their Impact on Ion Conductivity. *J. Am. Chem. Soc.* **2020**, *142*, 857−866.

(27) Park, J.; Staiger, A.; Mecking, S.; Winey, K. I. Structure-Property Relationships in Single-Ion Conducting Multiblock Copolymers: A Phase Diagram and Ionic Conductivities. *Macromolecules* **2021**, *54*, 4269−4279.

(28) Park, J.; Staiger, A.; Mecking, S.; Winey, K. I. Sub-3-Nanometer Domain Spacings of Ultrahigh-χ Multiblock Copolymers with Pendant Ionic Groups. *ACS Nano* **2021**, *15*, 16738−16747.

(29) Dolan, J. A.; Wilts, B. D.; Vignolini, S.; Baumberg, J. J.; Steiner, U.; Wilkinson, T. D. Optical Properties of Gyroid Structured Materials: From Photonic Crystals to Metamaterials. *Adv. Opt. Mater.* **2015**, *3*, 12−32.

(30) Hur, K.; Francescato, Y.; Giannini, V.; Maier, S. A.; Hennig, R. G.; Wiesner, U. Three-Dimensionally Isotropic Negative Refractive Index Materials from Block Copolymer Self-Assembled Chiral Gyroid Networks. *Angew. Chem., Int. Ed.* **2011**, *50*, 11985−11989.

(31) Choudhury, S.; Agrawal, M.; Formanek, P.; Jehnichen, D.; Fischer, D.; Krause, B.; Albrecht, V.; Stamm, M.; Ionov, L. Nanoporous Cathodes for High-Energy Li-S Batteries from Gyroid Block Copolymer Templates. *ACS Nano* **2015**, *9*, 6147−6157.

(32) Werner, J. G.; Rodríguez-Calero, G. G.; Abruña, H. D.; Wiesner, U. Block Copolymer Derived 3-D Interpenetrating Multi-

functional Gyroidal Nanohybrids for Electrical Energy Storage. *Energy Environ. Sci.* **2018**, *11*, 1261−1270.
(33) Wei, D.; Scherer, M. R. J.; Bower, C.; Andrew, P.; Ryhänen, T.; Steiner, U. A Nanostructured Electrochromic Supercapacitor. *Nano Lett.* **2012**, *12*, 1857−1862.
(34) Benoit, H.; Hadziioannou, G. Scattering Theory and Properties of Block Copolymers with Various Architectures in the Homogeneous Bulk State. *Macromolecules* **1988**, *21*, 1449−1464.
(35) Kuriyama, K.; Shimizu, S.; Eguchi, K.; Russell, T. P. Development of Poly(Imide-b-Amic Acid) Multiblock Copolymer Thin Film. *Macromolecules* **2003**, *36*, 4976−4982.
(36) Tsubakihara, S.; Nakamura, A.; Yasuniwa, M. Hexagonal Phase of Polyethylene Fibers under High Pressure. *Polym. J.* **1991**, *23*, 1317−1324.
(37) Trigg, E. B.; Stevens, M. J.; Winey, K. I. Chain Folding Produces a Multilayered Morphology in a Precise Polymer: Simulations and Experiments. *J. Am. Chem. Soc.* **2017**, *139*, 3747−3755.
(38) Lee, B.; Park, I.; Yoon, J.; Park, S.; Kim, J.; Kim, K. W.; Chang, T.; Ree, M. Structural Analysis of Block Copolymer Thin Films with Grazing Incidence Small-Angle X-Ray Scattering. *Macromolecules* **2005**, *38*, 4311−4323.
(39) Crossland, E. J. W.; Kamperman, M.; Nedelcu, M.; Ducati, C.; Wiesner, U.; Smilgies, D. M.; Toombes, G. E. S.; Hillmyer, M. A.; Ludwigs, S.; Steiner, U.; et al. A Bicontinuous Double Gyroid Hybrid Solar Cell. *Nano Lett.* **2009**, *9*, 2807−2812.
(40) Jiang, Z. GIXSGUI: A MATLAB Toolbox for Grazing-Incidence X-Ray Scattering Data Visualization and Reduction, and Indexing of Buried Three-Dimensional Periodic Nanostructured Films. *J. Appl. Crystallogr.* **2015**, *48*, 917−926.
(41) Tomita, S.; Urakawa, H.; Wataoka, I.; Sasaki, S.; Sakurai, S. Complete and Comprehensive Orientation of Cylindrical Microdomains in a Block Copolymer Sheet. *Polym. J.* **2016**, *48*, 1123−1131.
(42) Zhang, Y.; Dong, R.; Gabinet, U. R.; Poling-Skutvik, R.; Kim, N. K.; Lee, C.; Imran, O. Q.; Feng, X.; Osuji, C. O. Rapid Fabrication by Lyotropic Self-Assembly of Thin Nanofiltration Membranes with Uniform 1 Nanometer Pores. *ACS Nano* **2021**, *15*, 8192−8203.
(43) Jung, J.; Park, H. W.; Lee, S.; Lee, H.; Chang, T.; Matsunaga, K.; Jinnai, H. Effect of Film Thickness on the Phase Behaviors of Diblock Copolymer Thin Film. *ACS Nano* **2010**, *4*, 3109−3116.
(44) Shi, A. C.; Li, B. Self-Assembly of Diblock Copolymers under Confinement. *Soft Matter* **2013**, *9*, 1398−1413.
(45) Hsu, C. H.; Yue, K.; Wang, J.; Dong, X. H.; Xia, Y.; Jiang, Z.; Thomas, E. L.; Cheng, S. Z. D. Thickness-Dependent Order-to-Order Transitions of Bolaform-like Giant Surfactant in Thin Films. *Macromolecules* **2017**, *50*, 7282−7290.
(46) Ryu, I. H.; Kim, Y. J.; Jung, Y. S.; Lim, J. S.; Ross, C. A.; Son, J. G. Interfacial Energy-Controlled Top Coats for Gyroid/Cylinder Phase Transitions of Polystyrene-Block-Polydimethylsiloxane Block Copolymer Thin Films. *ACS Appl. Mater. Interfaces* **2017**, *9*, 17427−17434.
(47) Aissou, K.; Mumtaz, M.; Portale, G.; Brochon, C.; Cloutet, E.; Fleury, G.; Hadziioannou, G. Templated Sub-100-Nm-Thick Double-Gyroid Structure from Si-Containing Block Copolymer Thin Films. *Small* **2017**, *13*, 1603777.
(48) Park, S.; Kim, Y.; Lee, W.; Hur, S. M.; Ryu, D. Y. Gyroid Structures in Solvent Annealed PS-b-PMMA Films: Controlled Orientation by Substrate Interactions. *Macromolecules* **2017**, *50*, 5033−5041.
(49) Nowak, S. R.; Lachmayr, K. K.; Yager, K. G.; Sita, L. R. Stable Thermotropic 3D and 2D Double Gyroid Nanostructures with Sub-2-Nm Feature Size from Scalable Sugar−Polyolefin Conjugates. *Angew. Chem., Int. Ed.* **2021**, *60*, 8710−8716.

https://doi.org/10.1021/acscentsci.1c01594
ACS Cent. Sci. 2022, 8, 388−393